



## RESEARCH PAPER

# Chloroquine differentially modulates coronary vasodilation in control and diabetic mice

Qian Zhang<sup>1,2,4</sup> | Atsumi Tsuji-Hosokawa<sup>2</sup> | Conor Willson<sup>2</sup> | Makiko Watanabe<sup>2</sup> | Rui Si<sup>2</sup> | Ning Lai<sup>1,4</sup> | Ziyi Wang<sup>1,3,4</sup> | Jason X.-J. Yuan<sup>1,3</sup> | Jian Wang<sup>3,4</sup>  | Ayako Makino<sup>1,2,3</sup> 

<sup>1</sup>Department of Medicine, University of California, San Diego, La Jolla, California

<sup>2</sup>Department of Physiology, The University of Arizona, Tucson, Arizona

<sup>3</sup>Department of Medicine, The University of Arizona, Tucson, Arizona

<sup>4</sup>State Key Laboratory of Respiratory Disease, Guangzhou Institute of Respiratory Disease, The First Affiliated Hospital of Guangzhou Medical University, Guangzhou, China

## Correspondence

Ayako Makino, PhD, Department of Medicine, University of California, San Diego, 9500 Gilman Drive, La Jolla, CA 92093.  
Email: amakino@ucsd.edu

## Funding information

National Heart, Lung, and Blood Institute of the National Institutes of Health, Grant/Award Numbers: HL146764 and HL142214

**Background and Purpose:** Chloroquine is a traditional medicine to treat malaria. There is increasing evidence that chloroquine not only induces phagocytosis but regulates vascular tone. Few reports investigating the effect of chloroquine on vascular responsiveness of coronary arteries have been made. In this study, we examined how chloroquine affected endothelium-dependent relaxation in coronary arteries under normal and diabetic conditions.

**Experimental Approach:** We isolated coronary arteries from mice and examined endothelium-dependent relaxation (EDR). Human coronary endothelial cells and mouse coronary endothelial cells isolated from control and diabetic mouse (TALLYHO/Jng [TH] mice, a spontaneous type 2 diabetic mouse model) were used for the molecular biological or cytosolic NO and Ca<sup>2+</sup> measurements.

**Key Results:** Chloroquine inhibited endothelium-derived NO-dependent relaxation but had negligible effect on endothelium-derived hyperpolarization (EDH)-dependent relaxation in coronary arteries of control mice. Chloroquine significantly decreased NO production in control human coronary endothelial cells partly by phosphorylating eNOS<sup>Thr495</sup> (an inhibitory phosphorylation site of eNOS) and attenuating the rise of cytosolic Ca<sup>2+</sup> concentration after stimulation. EDR was significantly inhibited in diabetic mice in comparison to control mice. Interestingly, chloroquine enhanced EDR in diabetic coronary arteries by, specifically, increasing EDH-dependent relaxation due partly to its augmenting effect on gap junction activity in diabetic mouse coronary endothelial cells.

**Conclusions and Implications:** These data indicate that chloroquine affects vascular relaxation differently under normal and diabetic conditions. Therefore, the patients' health condition such as coronary macrovascular or microvascular disease, with or without diabetes, must be taken account into the consideration when selecting chloroquine for the treatment of malaria.

**Abbreviations:** CA, coronary artery; CQ, chloroquine; EC, endothelial cell; EDR, endothelium-dependent relaxation; EDH, endothelium-derived hyperpolarization; EDNO, endothelium-derived NO; FPIX, ferriprotoporphyrin IX; HCECs, human coronary endothelial cells; MCECs, mouse coronary endothelial cells; SMC, smooth muscle cell; SOCE, store-operated Ca<sup>2+</sup> entry; T2D, Type 2 diabetic; TH mouse, TALLYHO/Jng mouse; VDCC, voltage-dependent L-type Ca<sup>2+</sup> channel; Wt, wild type

## 1 | INTRODUCTION

**Chloroquine** (CQ), a 4-aminoquinoline derivative, is an antimalarial drug that has also been used to treat other diseases including lupus erythematosus, rheumatoid arthritis, and amoebiasis (Egan, 2001; Rees & Maibach, 1963). Chloroquine exhibits weak base charge with  $pK_a$  of 8.1 for the amino group at Position 7 and  $pK_2 = 10.1$  for the amino group on the alkyl side chain (Larsson & Tjalve, 1979). This base character of chloroquine is responsible for killing malaria by accumulating chloroquine in the parasite's acidic digestive vacuole, where the parasites degrade haemoglobin a major nutrient source of parasites. During degradation of haemoglobin, the level of ferriprotoporphyrin IX (FPIX) is also increased in the digestive vacuole. In the meantime, parasites biocrystallize FPIX dimers into inert hemozoin crystals to avoid cell lysis. Chloroquine in the digestive vacuole inhibits hemozoin formation, which leads to FPIX accumulation, membrane permeabilization and cell lysis (Fong & Wright, 2013). The basic nature of chloroquine causes it be concentrated in lysosomes (lysosomotropic action). After the accumulation of chloroquine in lysosomes, the pH of the lysosome will increase from 4 to 6 (Kalia & Dutz, 2007; Kutner, Breuer, Ginsburg, & Cabantchik, 1987) and result in inactivation of many enzymes in the lysosome such as proteases. This is the main cause of chloroquine-induced autophagy inhibition (Mauthe et al., 2018).

Recently, there is increasing evidence that chloroquine also regulates the function of vascular cells (Manson et al., 2014; Pestana, Oishi, Salistre-Araujo, & Rodrigues, 2015; Sai et al., 2014; Wu et al., 2017) and cardiac myocytes (Sanchez-Chapula, Salinas-Stefanon, Torres-Jacome, Benavides-Haro, & Navarro-Polanco, 2001; Tona, Ng, Akera, & Brody, 1990). Sai et al. (2014) demonstrated that chloroquine induces vasodilation in rat aorta at high concentration ( $>100 \mu\text{mol}\cdot\text{L}^{-1}$ ) via inhibiting voltage-dependent L-type  $\text{Ca}^{2+}$  channel (VDCC). We have also found that pretreatment with chloroquine ( $200 \mu\text{mol}\cdot\text{L}^{-1}$ ) attenuates vascular contraction in mouse pulmonary artery through inhibition of VDCC in smooth muscle cells (SMCs; Wu et al., 2017). Pestana et al. (2015) show that chloroquine relaxes vessels in a dose-dependent manner by increasing NO production in rat aorta. In contrast, Manson et al. (2014) demonstrate that chloroquine induces vasodilation independent of endothelium, VDCC, and  $\text{Ca}^{2+}$ -activated  $\text{K}^+$  channel in guinea pig aorta. These data suggest that the effect of chloroquine on vascular response varies in different tissues and organs. In this study, we have aimed to investigate the effect of chloroquine on vascular relaxation in coronary arteries (CAs) isolated from control and diabetic mice.

Chronic hyperglycaemia leads to cardiovascular complications that are a leading cause of death in diabetic patients. Endothelial cell (EC) dysfunction is a major cause of vascular complications in diabetes, while coronary endothelial dysfunction is implicated in the increased morbidity of coronary artery disease and coronary microvascular disease in diabetes (Belin de Chantemele & Stepp, 2012; Labazi & Trask, 2017; Pant, Marok, & Klein, 2014; Pepine et al., 2015; Rocic, 2012). It is therefore scientifically important and clinically relevant to examine whether chloroquine has a maladaptive effect on coronary endothelial function in diabetes. To the best of our knowledge, there is no report examining chloroquine effect on coronary vascular function in

### What is already known

- Chloroquine is a useful anti-malaria treatment but also serves as a regulator of vascular tone.
- There is no reports examining the effect of chloroquine on vascular response in coronary arteries.

### What this study adds

- Chloroquine attenuates EDR by reducing NO but not EDH in normal mice CAs.
- In diabetic mice, chloroquine enhances EDR via augmenting the activity of the gap junctions.

### What is the clinical significance

- Chloroquine should be used with caution in patients with non-diabetic cardiovascular disease.

diabetes, although chloroquine was examined on other organs of diabetics. Chloroquine appears to exert a beneficial effect in both insulin-dependent and insulin-independent diabetic patients (Blazar et al., 1984; Powrie et al., 1993; Smith, Amos, Mahler, & Peters, 1987) due partly to its inhibition of insulin degradation (Blazar et al., 1984). In diabetic animal models, chloroquine treatment significantly improves diastolic function of the left ventricle (Yuan et al., 2016), tubular function in the kidney (Jeong et al., 2018), and abnormal gluconeogenesis in the liver (Jarzyna, Kiersztan, Lisowa, & Bryla, 2001). Those data indicate that chloroquine might be a useful treatment to improve hyperglycaemia- and diabetes-induced complications. In this study, we were the first to examine the effect of chloroquine on endothelium-dependent relaxation (EDR) in CAs and compare the effect of chloroquine on coronary vasodilation in healthy and diabetic mice. We also determined the molecular mechanisms underlining these outcomes. The data show that chloroquine differentially affects coronary vascular function in healthy control and diabetic mice. The study provides important insights into the understanding of the adverse effect of chloroquine on coronary function in control patients or patients without diabetes.

## 2 | METHODS

### 2.1 | Animals

This study was conducted in accordance with the guidelines established by the Institutional Animal Care and Use Committee (IACUC) at the University of Arizona (UA) and University of California, San Diego (UCSD). All animal use is in compliance with all current U.S. government regulations concerning the care and use of laboratory animals. Animal studies are reported in compliance with the ARRIVE guidelines (Kilkenny, Browne, Cuthill, Emerson, & Altman, 2010) and with the recommendations made by the British Journal of

Pharmacology. The University has been certified by PHS with Animal Welfare Assurance numbers A3248-01 (UA) and A3033-01 (UCSD), and the approved IACUC protocol numbers for this study are 14-520 (UA) and S18185 (UCSD). The laboratory personnel who conducted following experiments took all the training required for animal handling and were certified by the IACUC.

TALLYHO/Jng (TH) mice were purchased from the Jackson Laboratory (Bar Harbor, Maine, USA; RRID:IMSR\_JAX:005314) and bred in our animal facility. The TH mouse is a polygenic type 2 diabetic (T2D) model, and we used C57BL/6 as a wild-type (Wt) control (Kim & Saxton, 2012). Male C57BL/6 mice (ENVIGO, Placentia, California, USA; RRID:MGI:2161078) were used at the age of  $\leq 16$  weeks in Figure 1. TH male mice were used at the age of 16–25 weeks, and the age-matched Wt mice were used as control. All mice were housed in a specific pathogen-free facility with five mice per cage and maintained at 23–25°C with 12-hr light–12-hr dark cycle and standard rodent diet and water ad libitum.

Mice were randomized to groups for each experiment. Oral glucose tolerance test (OGTT) and measurements of plasma cholesterol, HDL, triglyceride, and insulin levels were achieved as described in a previous paper (Cho, Basu, Dai, Heldak, & Makino, 2013). Heart dissection was performed under terminal anaesthesia with a mixture of ketamine (100 mg·kg<sup>-1</sup>, i.p.) and xylazine (5 mg·kg<sup>-1</sup>, i.p.). The body weight of mice used in this study was 29.2 ± 0.7 g in Wt mice and 35.2 ± 1.2 g in TH mice ( $P < .01$ ), and blood glucose levels without fasting were 172.3 ± 9.3 mg·dl<sup>-1</sup> in Wt mice and 422.9 ± 28.8 mg·dl<sup>-1</sup> in TH mice ( $P < .01$ ; Wt,  $n = 29$ ; TH,  $n = 28$ ).

## 2.2 | Determination of chloroquine concentration for the experiment

The concentration of chloroquine (Cat# C6628, Sigma-Aldrich Corp. St. Louis, MO, USA), which we used in this study, was determined based on the literature. It has been demonstrated that a plateau plasma

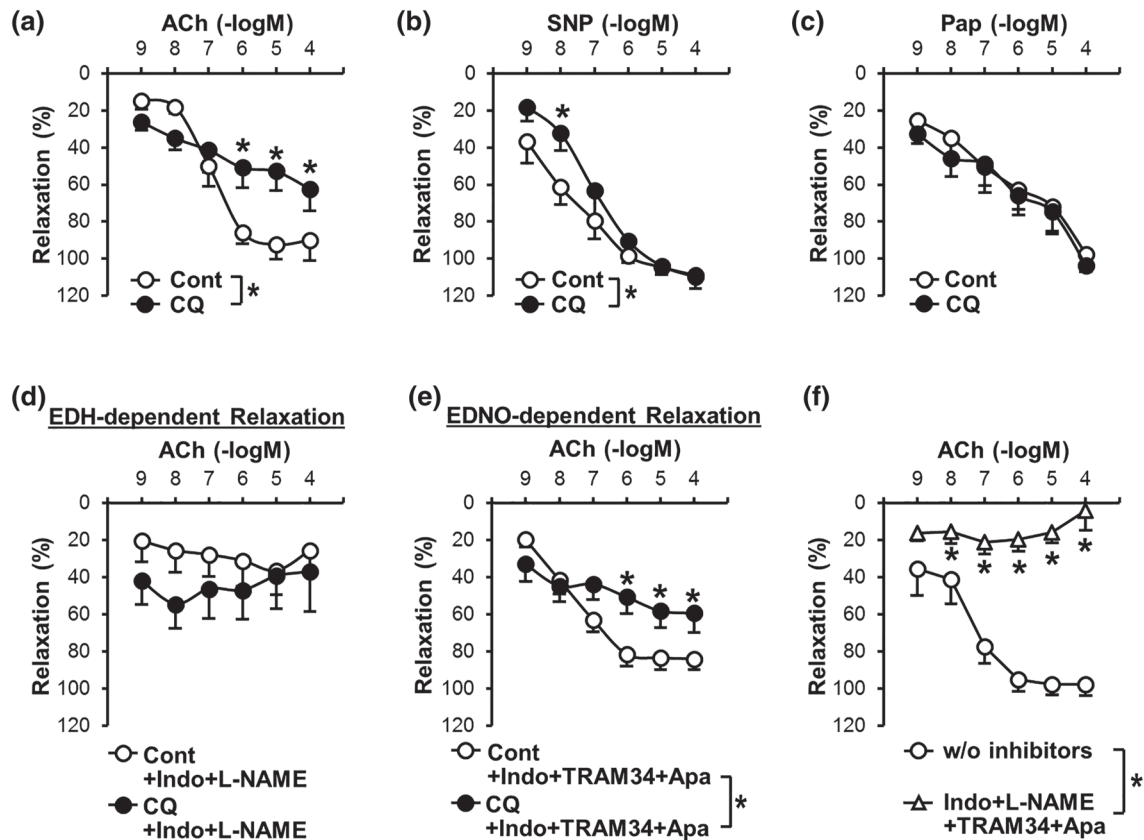


**FIGURE 1** Endothelium-dependent relaxation in coronary artery is attenuated by chloroquine. (a) Endothelium-dependent relaxation (EDR) induced by ACh in the absence (Cont, open circle) or presence (CQ, closed circle) of chloroquine (CQ, 10  $\mu$ M).  $n_{\text{mice}} = 6$  in each group. Data are mean  $\pm$  SE. \* $P < .05$  versus Cont. (b) Smooth muscle (SM)-dependent relaxation induced by sodium nitroprusside (SNP, an NO donor) in the absence (Cont) or presence (CQ) of CQ.  $n_{\text{mice}} = 7$  in each group. (c) SM-dependent relaxation induced by papaverine (Pap, a PDE inhibitor) in the absence (Cont) or presence (CQ) of CQ.  $n_{\text{mice}} = 6$  in each group. (d) Endothelium-derived hyperpolarization (EDH)-dependent relaxation in the absence (Cont) or presence (CQ) of CQ. EDH-dependent relaxation was conducted by ACh administration in the presence of indomethacin (Indo, a COX inhibitor, 10  $\mu$ M) and L-NAME (an eNOS inhibitor, 100  $\mu$ M).  $n_{\text{mice}} = 8$  in each group. (e) Endothelium-derived NO (EDNO)-dependent relaxation in the absence (Cont) or presence (CQ) of CQ. EDNO-dependent relaxation was accessed by ACh administration in the presence of Indo, TRAM34 (an inhibitor of intermediate-conductance Ca<sup>2+</sup>-activated K<sup>+</sup> channel, 100 nM), and apamin (an inhibitor of small conductance Ca<sup>2+</sup> activated K<sup>+</sup> channel, 100 nM).  $n_{\text{mice}} = 13$  in each group. (f) Pretreatment with Indo (to inhibit PGI<sub>2</sub>), L-NAME (to inhibit NO), and TRAM34 and apamin (to inhibit EDH) abolishes ACh-induced relaxation in coronary artery (CA).  $n_{\text{mice}} = 8$  in each group. \* $P < .05$  compared to control (i.e., w/o inhibitors). Statistical comparison between dose–response curves was made by two-way ANOVA with Bonferroni post hoc test

concentration is 10  $\mu\text{M}$  after administration of chloroquine at the dosage of 500  $\text{mg}\cdot\text{day}^{-1}$  and 1  $\mu\text{M}$  at 250  $\text{mg}\cdot\text{day}^{-1}$  (Mackenzie, 1983). Chloroquine is commonly administered at 100–250  $\text{mg}\cdot\text{kg}^{-1}$ , and 500 mg is the maximal dosage for daily administration (Mackenzie, 1983). The highest dosage is 1,500  $\text{mg}\cdot\text{day}^{-1}$  for 3 days for an acute episode of malaria (Reed & Campbell, 1962). Therefore, we used 10  $\mu\text{M}$  of chloroquine for our experiments. Chloroquine was dissolved in saline and freshly prepared at 10 mM before further dilution for the experiment.

### 2.3 | Isometric tension measurement in coronary arterial ring

Isometric tension was measured in isolated coronary arterial ring of mice to evaluate vascular function as previously described (Estrada et al., 2012; Makino, Platoshyn, Suarez, Yuan, & Dillmann, 2008). The heart was isolated from the mouse and put in modified Krebs–Henseleit solution (KHS) for dissection. The composition of KHS in mM: NaCl 118.0, KCl 4.7,  $\text{NaHCO}_3$  25.0,  $\text{CaCl}_2$  1.8,  $\text{NaH}_2\text{PO}_4$  1.2,  $\text{MgSO}_4$  1.2, and glucose 11.0. Third-order small coronary arteries were dissected, and adherent connective tissues and cardiac myocytes were removed. Arteries were cut into 1- to 1.5-mm segments. The arterial rings were mounted in a 4-channel wire myograph (620M, Danish Myo Technology A/S, Aarhus N, Denmark) over 20- $\mu\text{m}$  wires, set at a resting tension of 100 mg, and allowed to equilibrate for 45 min with intermittent washes every 15 min. After equilibration, each CA was contracted to achieve an active tension of about 50–100 mg (150–200 mg from the baseline) by treatment with  $\text{PGF}_{2\alpha}$ . The concentration of  $\text{PGF}_{2\alpha}$  used for precontraction was 1–10  $\mu\text{M}$ . The magnitude of contraction was  $76.5 \pm 6.1$  mg in Wt and  $66.2 \pm 11.8$  in TH. There was no statistical difference of  $\text{PGF}_{2\alpha}$ -induced contraction between Wt and TH. The degree of relaxation was shown as a percent of  $\text{PGF}_{2\alpha}$ -induced contraction.

The dose-dependent curve was generated using the raw data; averaged data were shown for each dose in the figure. The maximal response shown in the tables was calculated using the value at the maximal response of relaxation (or the maximal relaxation value).  $\text{EC}_{50}$  was calculated using Sigma Plot 12.5 (Systat Software, Inc., San Jose, CA, USA).

### 2.4 | Isolation of mouse coronary endothelial cell

Mouse coronary endothelial cell (MCECs) were isolated using a method previously described (Cho et al., 2013; Luo, Truong, & Makino, 2016; Makino et al., 2008; Makino et al., 2015).

### 2.5 | Cytosolic NO measurement

Cytosolic NO concentration ( $[\text{NO}]_{\text{cyto}}$ ) was measured using a modified method described in our previous paper (Estrada et al., 2012). Briefly, human coronary endothelial cells (HCECs, Cat# CC-2585, Lonza America, Inc., Alpharetta, GA, USA) were stained with DAF-FM diacetate (5  $\mu\text{M}$ ) for 30 min in the dark at room temperature. The DAF-FM-loaded cells were then washed and treated with chloroquine (10  $\mu\text{M}$ ) for 30 min. The fluorescent images of cells were obtained using an EVOS FL

Auto Imaging System (Thermo Fisher Scientific, Inc., Waltham, MA, USA). The background intensity of DAF-FM was subtracted from the cell intensity to precisely indicate the actual cell intensity of DAF-FM. The actual cell intensity in treated cells was then normalized to the actual cell intensity in non-treated cells to show changes of DAF-FM intensity.

### 2.6 | Cytosolic $\text{Ca}^{2+}$ measurement

Cytosolic-free  $\text{Ca}^{2+}$  concentration ( $[\text{Ca}^{2+}]_{\text{cyto}}$ ) in HCECs was measured using a modified method previously described (Estrada et al., 2012). Briefly, cells were plated on glass slides coated with 5% gelatine and loaded with the membrane-permeable acetoxymethyl ester form of fura 2 (fura2-AM; 4  $\mu\text{M}$  for 1 hr in the dark at room temperature). The fura2-AM-loaded cells were then superfused with physiological salt solution (PSS, pH 7.4, in mM: NaCl 141, KCl 4.7,  $\text{CaCl}_2$  1.8,  $\text{MgCl}_2$  1.2, HEPES 10, and glucose 10) for 30 min at 32°C. Fura-2 fluorescence signals from the cells and background were imaged using a Nikon TE300 microscope (Nikon Instruments, Inc., Melville, New York, USA). The changes in  $[\text{Ca}^{2+}]_{\text{cyto}}$  are described as a normalized ratio  $F/F_0$  ( $F = R_{340}/R_{380}$ ,  $F_0 =$  averaged  $F$  measured for 5 min before application of extracellular agonist). The amplitude of peak increase in  $[\text{Ca}^{2+}]_{\text{cyto}}$  ( $\Delta F/F_0$ ) and the AUC of the peak increase in  $[\text{Ca}^{2+}]_{\text{cyto}}$  per individual cells were measured and calculated. Data were normalized by the average of control data.

### 2.7 | Western blot analysis

Protein expression was analysed using an SDS-PAGE. Antibodies specifically against endothelial NOS (eNOS, 1:2000, sc-654, Santa Cruz Biotechnology, Inc., Dallas, TX, USA; RRID:AB\_631423), p-eNOS<sup>Ser1177</sup> (1:1000, #9570, Cell Signaling Technology, Danvers, MA, USA. RRID:AB\_823493), p-eNOS<sup>Thr495</sup> (1:1000, #9574, Cell Signaling Technology; RRID:AB\_2153176), and actin (1:4000, sc-1616, Santa Cruz Biotechnology, Inc., RRID:AB\_630836) were purchased from different companies as indicated above.

### 2.8 | Dye transfer assay

After MCEC isolation, cells were plated in a 24-well plate and cultured for 4 days to reach confluence. Cells were then incubated with chloroquine (10  $\mu\text{M}$ ) or vehicle (saline) for 30 min. Dye transfer assay was performed as described in our previous paper (Makino et al., 2015). Briefly, Lucifer yellow (0.5  $\text{mg}\cdot\text{ml}^{-1}$ ) was added to the well after chloroquine treatment, and the confluent cells were scratched by a scalpel in the middle of the well to allow dye to get into cells at the edge of the scrape. The dye solution was left for 20 min in the well, and then cells were washed and fixed. Images of dye transfer were captured using an EVOS FL Auto Imaging System. The distance of dye transfer from the scraping site to the farthest site of cells showing visual uptake of dye was measured using Image Pro-Plus 7.0 software (Media Cybernetics, Inc., Rockville, MD, USA). The data were normalized to the averaged distance of dye transfer in Wt cells without chloroquine treatment.

## 2.9 | Data analysis

The data and statistical analysis comply with the recommendations of the *British Journal of Pharmacology* on experimental design and analysis in pharmacology. We conducted data analysis in a blinded fashion whenever possible and set proper controls for every experimental

plan. The mouse numbers and independent experiment numbers are described in the figure legend.

Statistical analysis was performed using GraphPad Prism 8.1.2 (GraphPad Software, Inc., La Jolla, CA, USA; RRID:SCR\_002798). Data are presented as mean  $\pm$  SE. Student's *t* test was used for comparisons of two experimental groups (except Figure 2f,g), and one-way ANOVA

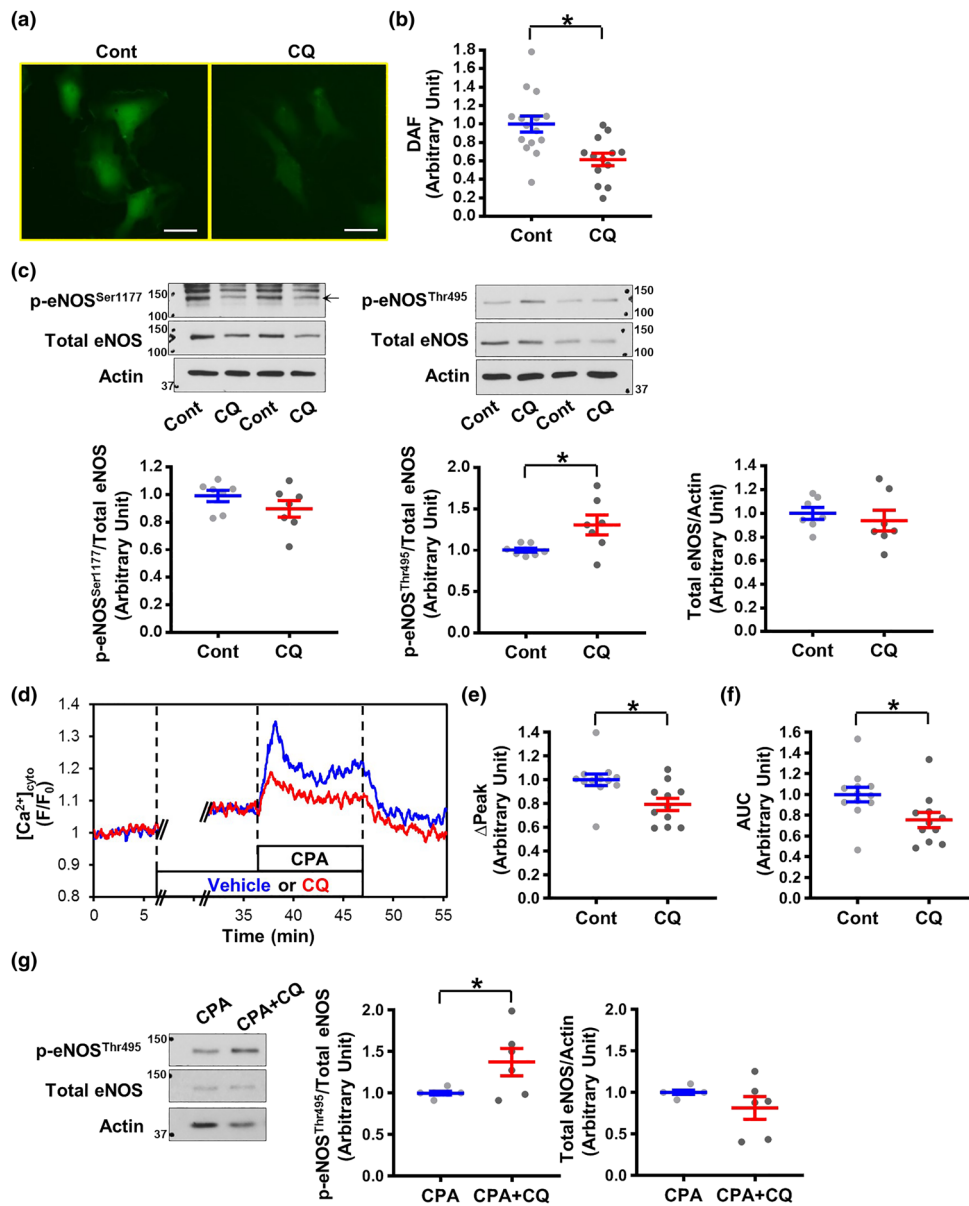


**FIGURE 2** CQ decreases cytosolic NO level, increases phosphorylated eNOS<sup>495</sup>, and attenuates the rise in cytosolic Ca<sup>2+</sup> concentration after stimulation in human coronary endothelial cells. (a) Representative images showing NO signals, determined by DAF, in human coronary endothelial cells (HCECs) with or without (w/o) CQ treatment for 30 min. Bar = 50  $\mu$ m. (b) Summarized data showing DAF intensity in control cells (Cont,  $n_{\text{experiment}} = 15$ ,  $n_{\text{cells}} = 127$ ) and CQ-treated cells (CQ,  $n_{\text{experiment}} = 13$ ,  $n_{\text{cells}} = 118$ ). Data are mean  $\pm$  SE. \* $P < .05$  compared to Cont. (c) WB analysis on total eNOS, phosphorylated eNOS at Ser1177 (p-eNOS<sup>Ser1177</sup>), and Thr495 (p-eNOS<sup>Thr495</sup>) in control HCECs (Cont) and CQ-treated HCECs (CQ). Actin was used as a loading control. The scattered plots show the level of p-eNOS normalized to total eNOS (left panels) and the level of total eNOS normalized to actin (right panel).  $n_{\text{experiment}} = 7$ . Data are mean  $\pm$  SE. \* $P < .05$  compared to Cont. (d) Representative records showing cytosolic Ca<sup>2+</sup> concentration ([Ca<sup>2+</sup>]<sub>cyto</sub>) in HCECs before, during, and after stimulation with cyclopiazonic acid (CPA, an inhibitor of sarcoplasmic reticulum Ca<sup>2+</sup>-ATPase to increase [Ca<sup>2+</sup>]<sub>cyto</sub>, 10  $\mu$ M) in the absence (vehicle, blue tracing) or presence (CQ, red tracing) of CQ. (e,f) Summarized data showing the amplitude ( $\Delta$ Peak, e) and the AUC (f) of CPA-induced increase in [Ca<sup>2+</sup>]<sub>cyto</sub> in control cells (Cont,  $n_{\text{experiment}} = 12$ ,  $n_{\text{cells}} = 120$ ) and CQ-treated cells (CQ,  $n_{\text{experiment}} = 11$ ,  $n_{\text{cells}} = 110$ ). Data are mean  $\pm$  SE. \* $P < .05$  compared to Cont. (g) The level of p-eNOS<sup>Thr495</sup> after the treatment of CPA with or without CQ.  $n_{\text{experiment}} = 6$ . Data are mean  $\pm$  SE. \* $P < .05$  compared to CPA. Unpaired Student's *t*-test was used for comparisons of two experimental groups in Figure 2b,c,g. Mann-Whitney test was used for Figures 2e,f

was used for multiple comparisons. Mann–Whitney test was used for Figure 2f,g. Statistical comparison between dose–response curves was made by a two-way ANOVA and a post hoc test with the Bonferroni correction (if  $F$  achieved the necessary level of statistical significance ( $P < 0.05$ ) and there is no significant variance in homogeneity). Differences were considered to be statistically significant when  $P$  value was less than .05 ( $*P < .05$ ).

## 2.10 | Materials

Ketamine and xylazine were purchased from Henry Schein Inc. (Melville, NY, USA). DAF-FM diacetate (Cat# D23844), Fura2-AM (Cat# F1221), and Lucifer yellow (Cat# L453) were purchased from Thermo Fisher Scientific Inc., Waltham, MA, USA. Other chemicals were obtained from Sigma-Aldrich Corp. St. Louis, MO, USA.

## 2.11 | Nomenclature of targets and ligands

Key protein targets and ligands in this article are hyperlinked to corresponding entries in <http://www.guidetopharmacology.org>, the common portal for data from the IUPHAR/BPS Guide to PHARMACOLOGY (Harding et al., 2018), and are permanently archived in the Concise Guide to PHARMACOLOGY 2017/18 (Alexander, Fabbro et al., 2017; Alexander, Christopoulos et al., 2017).

## 3 | RESULT

### 3.1 | Chloroquine attenuates EDR in coronary artery

Acetylcholine (ACh) induces EDR via releasing NO and prostacyclin and/or by hyperpolarizing cells. We first examined whether chloroquine affected endothelium-dependent coronary vasodilation. ACh was administered to CAs in a dose-dependent manner to evaluate the function of ECs. Pretreatment with chloroquine significantly attenuated ACh-induced vasodilation in CAs (Figure 1a and Table 1). In contrast, chloroquine had negligible effect on coronary vasodilation induced by sodium nitroprusside (SNP, an NO donor; Figure 1b) and papaverine (Pap, a PDE inhibitor; Figure 1c). These data indicate that chloroquine

significantly inhibits EDR but has no effect on endothelium-independent and smooth muscle (SM)-dependent vasodilation in CAs.

To examine the potential mechanisms involved in chloroquine-mediated inhibition of EDR, we used different chemicals to block each signalling cascade. We pretreated vessels with L-NAME (an eNOS inhibitor, 100  $\mu$ M) and indomethacin (Indo, a COX inhibitor, 10  $\mu$ M) to visualize endothelium-derived hyperpolarization (EDH)-dependent relaxation. We used a combination cocktail of apamin (Apa, an inhibitor of small-conductance  $Ca^{2+}$ -activated  $K^+$  [ $SK_{Ca}$ ] channel, 100 nM) and TRAM34 (an inhibitor of intermediate-conductance  $Ca^{2+}$ -activated  $K^+$  [ $IK_{Ca}$ ] channel, 100 nM) to inhibit EDH-dependent relaxation. In the presence of Apa, TRAM34, and Indo, we were able to observe endothelium-derived NO (EDNO)-dependent relaxation in isolated CAs. Chloroquine treatment did not affect EDH-dependent relaxation in CAs (Figure 1d), while chloroquine significantly attenuated EDNO-dependent relaxation (Figure 1e and Table 1). Figure 1f demonstrates that the treatment of Indo, L-NAME, Apa, and TRAM34 abolished EDR in CAs, confirming that ACh relaxes CAs through EDNO-, EDH-, and prostacyclin-dependent relaxation. These data indicate that chloroquine attenuates EDR in CAs due primarily to its inhibitory effect on EDNO-dependent relaxation, but not EDH-dependent relaxation.

### 3.2 | Chloroquine inhibits NO production in HCECs

To examine whether chloroquine-mediated inhibition on EDNO-dependent relaxation in CAs is, at least in part, due to its inhibitory effect on NO production in ECs, we measured and compared  $[NO]_{cyto}$  in HCECs and chloroquine-treated HCECs. We stained HCECs with DAF-FM to measure  $[NO]_{cyto}$ . Cells were then treated with vehicle (saline) or chloroquine for 30 min, and the DAF-FM image was taken and used to calculate  $[NO]_{cyto}$ . Figure 2a,b shows that chloroquine significantly decreased  $[NO]_{cyto}$  in HCECs. To examine the molecular mechanism by which chloroquine decreases  $[NO]_{cyto}$ , we examined and compared the eNOS activity in vehicle and chloroquine-treated HCECs. The levels of total eNOS and phosphorylated (p)-eNOS<sup>Ser1177</sup> (a positive regulatory site) were not altered by chloroquine, whereas the level of p-eNOS<sup>Thr495</sup> (a negative regulatory site) was significantly increased by chloroquine (Figure 2c). These data suggest that chloroquine may reduce the resting level of NO production by phosphorylation of eNOS at the negative regulatory site (Thr495).

**TABLE 1** Maximal responses and  $EC_{50}$  values of agonist-induced vasodilation in the absence or presence of chloroquine in mouse coronary arteries

		n	Vehicle		Chloroquine (CQ)	
			Max. (%)	-log ( $EC_{50}$ )	Max. (%)	-log ( $EC_{50}$ )
ACh	Untreated	6	93.9 $\pm$ 8.4	7.0 $\pm$ 0.1	64.7 $\pm$ 11.0*	7.4 $\pm$ 0.7
	L-NAME + Indo	7	49.9 $\pm$ 11.0	6.2 $\pm$ 0.6	75.9 $\pm$ 10.3*	7.1 $\pm$ 0.5
	TRAM34 + Apa + Indo	13	86.3 $\pm$ 6.2	7.8 $\pm$ 0.3	64.9 $\pm$ 9.1*	7.7 $\pm$ 0.5
SNP	Untreated	7	108.9 $\pm$ 3.7	9.2 $\pm$ 0.9	109.9 $\pm$ 6.1	7.0 $\pm$ 0.4
Pap	Untreated	6	98.0 $\pm$ 8.0	6.2 $\pm$ 0.8	103.7 $\pm$ 3.5	6.0 $\pm$ 0.5

Note. L-NAME, 100  $\mu$ M; Indo, 10  $\mu$ M; TRAM34, 100 nM; Apa, 100 nM. Data are mean  $\pm$  SE.

\* $P < .05$  compared to vehicle.

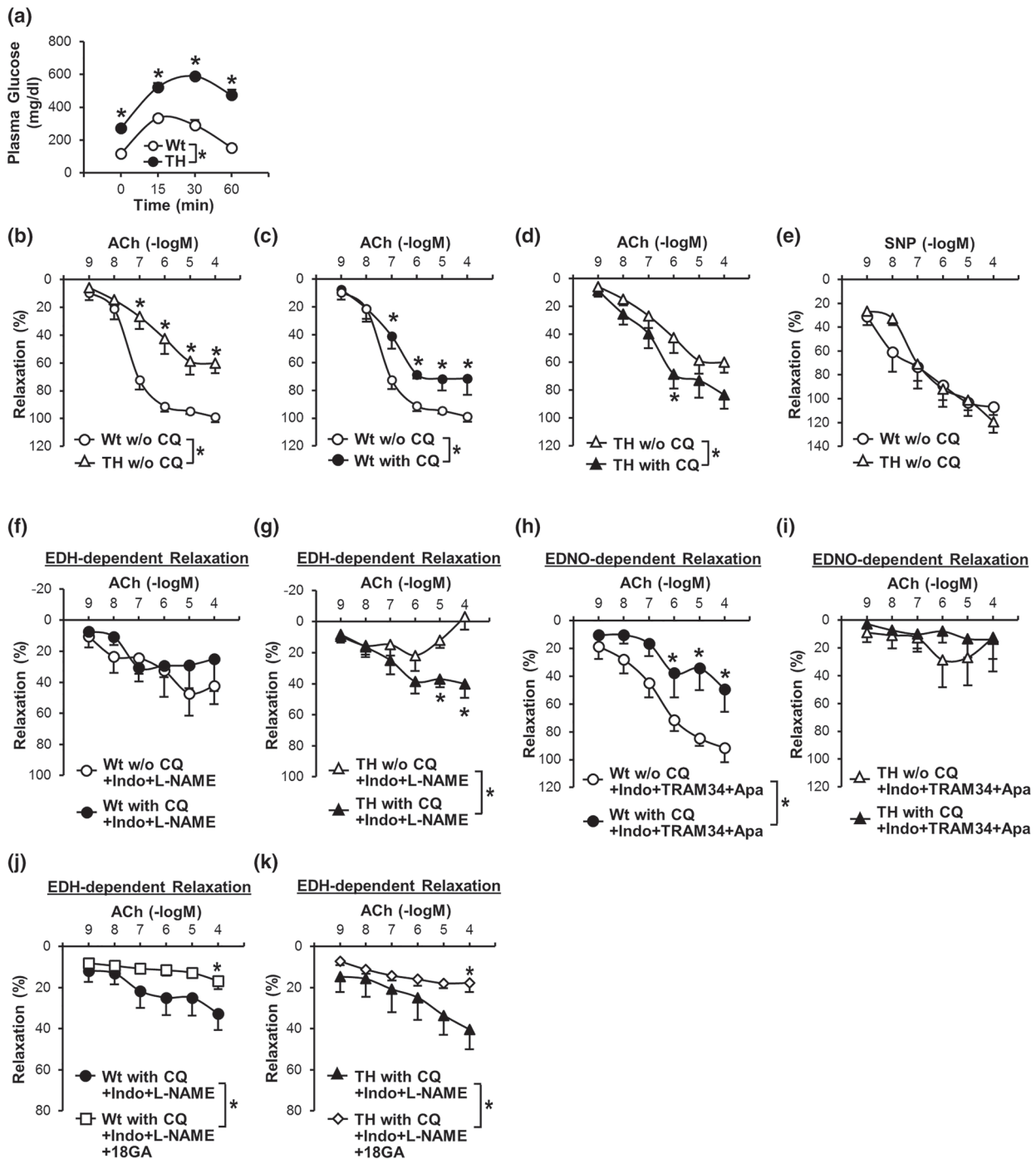


**FIGURE 3** CQ enhances EDH-dependent coronary vasodilation in diabetic mice. (a) Oral glucose tolerance test in Wt mice ( $n_{mice} = 7$ ) and TH mice ( $n_{mice} = 7$ ). \* $P < .05$  compared to Wt mice. (b) EDR in CAs from Wt and TH mice without CQ treatment (w/o CQ). Wt w/o CQ,  $n_{mice} = 13$ ; TH w/o CQ,  $n_{mice} = 12$ . Data are mean  $\pm$  SE. \* $P < .05$  compared to Wt w/o CQ. (c) Effect of CQ on EDR in CAs from Wt mice. Wt w/o CQ,  $n_{mice} = 13$ ; Wt with CQ,  $n_{mice} = 9$ . Data are mean  $\pm$  SE. \* $P < .05$  compared to Wt w/o CQ. (d) Effect of CQ on EDR in CAs from TH mice. TH w/o CQ,  $n_{mice} = 12$ ; TH with CQ,  $n_{mice} = 8$ . Data are mean  $\pm$  SE. \* $P < .05$  compared to TH w/o CQ. (e) SM-dependent relaxation induced by SNP in CAs from Wt ( $n_{mice} = 5$ ) and TH mice ( $n_{mice} = 5$ ) in the absence of CQ treatment (w/o CQ). (f) EDH-dependent relaxation in CAs isolated from Wt mice in the absence or presence of CQ.  $n_{mice} = 7$  in each group. \* $P < .05$  compared to w/o CQ. (g) EDH-dependent relaxation in CAs from TH mice in the absence or presence of CQ.  $n_{mice} = 7$  in each group. \* $P < .05$  versus w/o CQ. (h) EDNO-dependent relaxation in CAs from Wt mice in the absence or presence of CQ.  $n_{mice} = 6$  in each group. \* $P < .05$  versus w/o CQ. (i) EDNO-dependent relaxation in CAs from TH mice in the absence or presence of CQ.  $n_{mice} = 5$  in each group. Indo and L-NAME were used to inhibit  $PGI_2$  and NO in experiments shown in (f) and (g), while Indo, TRAM34, and apamin were used to inhibit  $PGI_2$  and EDH in experiments shown in (h) and (i). (j) EDH-dependent relaxation in CAs isolated from Wt mice in the presence of CQ with vehicle (0.25% ethanol) or 18GA (a non-specific Gap junction inhibitor, 50  $\mu$ M).  $n_{mice} = 8$  in each group. (k) EDH-dependent relaxation in CAs from TH mice in the presence of CQ with vehicle or 18GA.  $n_{mice} = 8$  in each group. \* $P < .05$  versus w/o 18GA. Statistical comparison between dose-response curves were made by two-way ANOVA with Bonferroni post hoc test

### 3.3 | Chloroquine pretreatment attenuates the increase in $[Ca^{2+}]_{cyto}$ after stimulation in HCECs

Since an increase in  $[Ca^{2+}]_{cyto}$  leads to eNOS activation and induces NO production, we examined the effect of chloroquine on the rise of  $[Ca^{2+}]_{cyto}$  after stimulation. **Cyclopiazonic acid** (CPA, an inhibitor of sarcoplasmic reticulum  $Ca^{2+}$ -ATPase) was used to increase  $[Ca^{2+}]_{cyto}$  by inducing store-operated  $Ca^{2+}$  entry (SOCE). Chloroquine treatment did not affect the resting level of  $[Ca^{2+}]_{cyto}$  (vehicle,  $1.14 \pm 0.06$ ; chloroquine,  $1.14 \pm 0.02$ ,  $P = .98$ ) but significantly inhibited CPA-induced increase in  $[Ca^{2+}]_{cyto}$  (Figure 2d–f). In addition, we found that chloroquine still increased the level of p-eNOS<sup>Thr495</sup> in the presence of CPA (Figure 2g), implying that NO production was decreased by chloroquine due to attenuated  $Ca^{2+}$  influx and increased p-eNOS<sup>Thr495</sup> level.

### 3.4 | Chloroquine enhances EDH-dependent relaxation in CAs of diabetic mice

To examine the effect of chloroquine on coronary vasodilation in diabetes, we used CAs dissected from control Wt mice and diabetic TH mice, a well-established T2D mouse model with abnormal glucose tolerance (Figure 3a), hyperinsulinaemia, and dyslipidaemia (Table 2). EDR was significantly attenuated in CAs from diabetic mice compared to CAs from control mice (Figure 3b), whereas there was no difference of SM-dependent relaxation in CAs dissected from control and diabetic mice (Figure 3e). Chloroquine significantly attenuated EDR in CAs from control mice (Figure 3c) but enhanced EDR in CAs from diabetic mice (Figure 3d). The chloroquine-mediated inhibition of EDR, which we observed in CAs from control mice, was due obviously to the attenuated EDNO-dependent relaxation (Figure 3h), but not to EDH-dependent relaxation (Figure 3f). The chloroquine-mediated augmentation of EDR, which we observed in CAs from diabetic mice, resulted from increased EDH-dependent relaxation (Figure 3g). Chloroquine had a negligible effect on EDNO-dependent relaxation in CAs from diabetic mice (Figure 3i). We also examined the effect of 18 $\beta$ -glycyrrhetic acid (18GA, a non-specific gap junction inhibitor, 50  $\mu$ M) on EDH-dependent relaxation in the presence of chloroquine (Figure 3j,k). CAs were pre-incubated with chloroquine and 18GA or

vehicle (0.25% ethanol) for 30 min before preconstruction. Enhanced EDH-dependent relaxation was significantly attenuated by 18GA treatment in control and diabetic mice. These data suggest that augmented EDH-dependent relaxation by chloroquine was due partly to increased gap junction activity in diabetic mice (Table 3).

### 3.5 | Chloroquine enhances gap junction activity in MCECs isolated from diabetic mice

To confirm that chloroquine regulates gap junction activity, we examined the effect of chloroquine on endothelial gap junctions in coronary ECs (MCECs) isolated from control and diabetic mice. Gap junction activity was assessed by the dye transfer experiment (Makino et al., 2015). Figure 4a,b demonstrates that the distance of dye transfer was significantly decreased in MCECs isolated from diabetic mice compared to MCECs from control mice and chloroquine significantly increased the distance of dye transfer in MCECs of diabetic mice. These data indicate that chloroquine enhances gap junction activity in diabetic MCECs and subsequently enhances EDH-dependent relaxation in CAs of diabetic mice.

### 3.6 | Chloroquine pretreatment did not affect the increase in $[Ca^{2+}]_{cyto}$ after stimulation in MCECs isolated from diabetic mice

To examine whether chloroquine differentially regulates  $Ca^{2+}$  influx between control and diabetes, we isolated MCECs from control and diabetic mice and conducted digital imaging fluorescence microscopy experiments to measure CPA-induced  $[Ca^{2+}]_{cyto}$  changes in the presence or absence of chloroquine. CPA was used to induce SOCE as illustrated in Figure 2a. CPA-induced  $[Ca^{2+}]_{cyto}$  increase was significantly decreased by chloroquine treatment in MCECs from control mice; however, there was no difference of CPA-induced  $[Ca^{2+}]_{cyto}$  increase in the presence or absence of chloroquine in MCECs from diabetic mice (Figure 4c,d). These data suggest that enhanced EDH-dependent relaxation in diabetic mice is due mainly to increased gap junction activity, but not to changing  $[Ca^{2+}]_{cyto}$  in MCECs.

**TABLE 2** Pharmacological parameters of Wt and TH mice

	Wt (n = 8)	TH (n = 8)
Body weight (g)	27.9 $\pm$ 0.5	32.8 $\pm$ 1.8*
Blood glucose (mg·L <sup>-1</sup> )	1633 $\pm$ 150	5388 $\pm$ 278*
Insulin (ng·mL <sup>-1</sup> )	0.19 $\pm$ 0.03	0.48 $\pm$ 0.11*
TC (mg·L <sup>-1</sup> )	806 $\pm$ 35	1536 $\pm$ 45*
HDL (mg·L <sup>-1</sup> )	412 $\pm$ 40	719 $\pm$ 37*
TG (mg·L <sup>-1</sup> )	306 $\pm$ 72	1614 $\pm$ 695*
LDL/VLDL (mg·L <sup>-1</sup> )	333 $\pm$ 59	494 $\pm$ 102

Note. Data are mean  $\pm$  SE.

Abbreviations: TC, plasma total cholesterol; TG, plasma triglyceride.

\* $P < .05$  compared to Wt.

## 4 | DISCUSSION

The vascular response to the same agonist is not always the same among different organs and branches of vessels. Although there are several studies investigating the effect of chloroquine on vascular response (Manson et al., 2014; Pestana et al., 2015; Sai et al., 2014; Wu et al., 2017), there is no report so far that examines the effect of chloroquine on vasodilation in CAs isolated from healthy and diabetic mice. Muscarinic agonist (e.g. ACh) and  **$\alpha$ 2-adrenoceptor agonist** induce EDR in all types of vessels; however, EDR in the large proximal artery is caused primarily by releasing NO from the endothelium, while EDH-dependent vasodilation is prominent in small distal artery (Garland & Dora, 2017; Godo et al., 2016) because of more myoendothelial gap junctions in smaller vessels than in large vessels



**TABLE 3** Maximal responses and EC<sub>50</sub> values of agonist-induced vasodilation in the absence or presence of chloroquine (CQ) in mouse coronary arteries dissected from Wt or TH mice

		Wt				TH			
		n	Vehicle	n	CQ	n	Vehicle	n	CQ
Max. response									
ACh	Untreated	13	101.6 ± 2.8	9	84.4 ± 5.1*	12	66.1 ± 8.1	8	85.8 ± 9.8
	L-NAME + Indo	7	55.3 ± 14.3	7	45.3 ± 16.1	7	27.5 ± 9.9	7	53.7 ± 5.0*
	TRAM34 + Apa + Indo	6	93.0 ± 9.6	6	51.1 ± 17.0*	5	35.4 ± 19.0	5	19.7 ± 13.2
SNP	Untreated	5	107.1 ± 7.0			5	119.5 ± 9.1		
-log (EC <sub>50</sub> )									
ACh	Untreated	13	7.5 ± 0.3	9	7.0 ± 0.3	12	6.6 ± 0.3	8	7.1 ± 0.5
	L-NAME + Indo	7	7.4 ± 0.6	7	7.6 ± 0.4	7	8.2 ± 0.8	7	6.4 ± 0.5*
	TRAM34 + Apa + Indo	6	7.6 ± 0.7	6	6.0 ± 0.5	5	6.0 ± 0.4	5	8.7 ± 0.1*
SNP	Untreated	5	7.7 ± 0.5			5	6.7 ± 0.4		
		n	Vehicle	n	18GA	n	Vehicle	n	18GA
Max. response									
ACh	L-NAME + Indo + CQ	8	37.1 ± 8.5	8	18.2 ± 3.6	8	41.9 ± 9.6	8	23.1 ± 3.2
-log (EC <sub>50</sub> )									
ACh	L-NAME + Indo + CQ	8	5.4 ± 0.4	8	8.1 ± 0.8*	8	6.1 ± 0.6	8	8.4 ± 0.8*

Note. L-NAME, 100 μM; Indo, 10 μM; TRAM34, 100 nM; Apa, 100 nM; vehicle for CQ, saline; 18GA, 50 μM; vehicle for 18GA, 0.25% ethanol. Data are mean ± SE.

\**P* < .05 versus vehicle.

(Hill, Rummery, Hickey, & Sandow, 2002; Sandow & Hill, 2000; Straub, Zeigler, & Isakson, 2014). In this study, we used small CAs (third order), which enabled us to examine both EDH-dependent and EDNO-dependent vascular relaxation. Changes in EDH-dependent relaxation in small distal arteries also play a critical role under pathophysiological conditions (i.e., coronary microvascular disease). In control mice, chloroquine attenuated EDR in CAs via inhibition of EDNO-dependent relaxation (instead of EDH-dependent relaxation; Figure 1). Both SNP and Pap lead to vascular relaxation by increasing cGMP in SMCs, and chloroquine did not affect SNP- and Pap-induced vascular relaxation, suggesting that chloroquine attenuates NO-dependent relaxation by altering EC function without changing SMC function. The chloroquine-mediated inhibition of EDNO-dependent relaxation could result from reduced NO production or decreased NO bioavailability in ECs. Figure 2b shows that NO concentration in HCECs is significantly decreased by chloroquine treatment. In our pilot study, we measured cytosolic ROS using DHE staining (Makino, Scott, & Dillmann, 2010) and found no change of DHE intensity after the treatment of chloroquine (Control, 9.97 ± 1.50 [*n*<sub>cell</sub> = 135, *n*<sub>experiment</sub> = 12]; chloroquine, 8.55 ± 1.46 [*n*<sub>cell</sub> = 122, *n*<sub>experiment</sub> = 12]; *P* > .05). These data suggest that the chloroquine -induced attenuation of EDNO-dependent relaxation is more likely due to the decrease in NO production.

eNOS activation is regulated by phosphorylation and cofactors binding. Several phosphorylation sites in eNOS differentially regulate the activity of eNOS. Among those sites, Ser1177 and Thr495 are the two most studied phosphorylation sites in eNOS (Rafikov et al., 2011). Ser1177 is not phosphorylated under resting condition, and a rise of [Ca<sup>2+</sup>]<sub>cyto</sub> phosphorylates Ser1177 via CaMKII activation and

increases NO production. On the other hand, Thr495 is a negative regulatory site for which phosphorylation leads to a decrease in eNOS activity. Chloroquine treatment in ECs significantly increased p-eNOS<sup>Thr495</sup> without changing p-eNOS<sup>Ser1177</sup> (Figure 2c), suggesting that NO production might be reduced by increasing p-eNOS<sup>Thr495</sup> level. After binding of ACh to the muscarinic receptor, [Ca<sup>2+</sup>]<sub>cyto</sub> is increased through Ca<sup>2+</sup> release from the endoplasmic reticulum, which activates eNOS via Ca<sup>2+</sup>/calmodulin binding. Therefore, inhibition of agonist-induced increase in [Ca<sup>2+</sup>]<sub>cyto</sub> causes the reduction of NO production. In this study, we used CPA to increase [Ca<sup>2+</sup>]<sub>cyto</sub> by depleting intracellular Ca<sup>2+</sup> stores and causing SOCE. The number of ACh receptor in ECs is often decreased each day after the isolation, and it is difficult to get homogenous response to ACh from isolated ECs (Tracey & Peach, 1992). However, isolated MCECs respond to CPA and lead to SOCE in all cells (Estrada et al., 2012). We found that chloroquine significantly inhibited CPA-induced rise in [Ca<sup>2+</sup>]<sub>cyto</sub> (Figure 2d–f). The data in Figure 2 suggest that chloroquine attenuates NO production via reducing eNOS activity through increasing p-eNOS<sup>Thr495</sup> and inhibiting the rise of [Ca<sup>2+</sup>]<sub>cyto</sub>. However, we do not know how chloroquine phosphorylates Thr495 in eNOS or how chloroquine decreases Ca<sup>2+</sup> influx. Further studies are needed to define the mechanisms involved in chloroquine-mediated phosphorylation of p-eNOS<sup>Thr495</sup> and decrease in SOCE.

Change of [Ca<sup>2+</sup>]<sub>cyto</sub> may also affect EDH-dependent vascular relaxation via reducing activation of SK<sub>Ca</sub> channel and IK<sub>Ca</sub> channels. However, we did not see a decrease in EDH-dependent relaxation by chloroquine treatment; we actually observed a slight increase of relaxation in control mice (Figure 1d). In the absence of extracellular

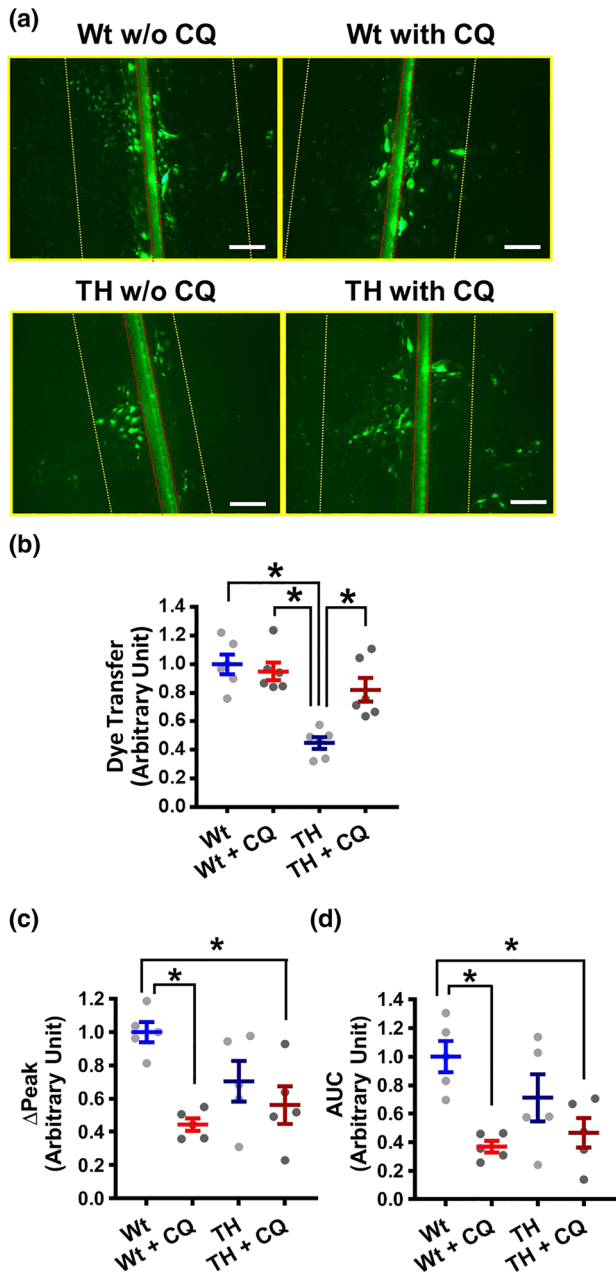


**FIGURE 4** CQ increases gap junction activity but does not change the CPA-induced  $[Ca^{2+}]_{cyto}$  increase, in MCECs isolated from TH mice. (a,b) Lucifer yellow dye transfer experiment in MCECs was conducted to examine the gap junction activity. (a) Representative photographs showing the images of LY dye transfer in ECs. The red line indicates the edge of the scrape. The yellow line indicates the farthest site of cells showing visual uptake of dye. The distance between yellow and red lines was calculated as a dye transfer. (b) The scattered dots show the normalized data of dye transfer by the distance in MCECs isolated from Wt without CQ (Wt-MCECs w/o CQ). Bar = 100  $\mu$ .  $n_{mice} = 6$  in each group. (c,d) Summarized data showing  $\Delta$ Peak (c) and the AUC (d) of CPA-induced increase in  $[Ca^{2+}]_{cyto}$  in Wt MCECs w/o CQ (Wt,  $n_{mice} = 5$ ,  $n_{cells} = 43$ ), Wt MCECs with CQ (Wt + CQ,  $n_{mice} = 5$ ,  $n_{cells} = 43$ ), TH MCECs w/o CQ (TH,  $n_{mice} = 5$ ,  $n_{cells} = 44$ ), and TH MCECs with CQ (TH + CQ,  $n_{mice} = 5$ ,  $n_{cells} = 44$ ). \* $P < .05$  between groups as indicated. Statistical comparison between the groups was made by one-way ANOVA with Bonferroni post hoc test

$Ca^{2+}$  or in the presence of **nifedipine** (a selective blocker of L-type voltage-dependent  $Ca^{2+}$  channels), ACh can still evoke membrane hyperpolarization in SMCs (Chen & Suzuki, 1990; Fukao, Hattori, Kanno, Sakuma, & Kitabatake, 1997). In addition, some endothelium-derived hyperpolarization factors (EDHFs) can directly relax smooth muscle without activating  $SK_{Ca}$  and  $IK_{Ca}$  channels in ECs (Campbell & Fleming, 2010; O'Sullivan, Kendall, & Randall, 2004; Zhang et al., 2012). Therefore, it is possible that decreased CPA-induced rise in  $[Ca^{2+}]_{cyto}$  after chloroquine treatment might not be sufficient to attenuate EDH-dependent relaxation in control mice.

Diabetic patients exhibit a higher morbidity of malaria infection (Danquah, Bedu-Addo, & Mockenhaupt, 2010); however, less information is available about the effect of the antimalarial drug on cardiovascular complications in diabetes. Major diabetic complications associated with morbidity are coronary artery and coronary microvascular disease. Ischaemia due to coronary artery disease is caused by occlusion or narrowing vessels as a result of lipid plaque formation, whereas the patient with coronary microvascular disease shows a clear angiograph with reduced coronary flow due to attenuated relaxation in the distal artery and reduced number of capillaries. Coronary endothelial dysfunction is implicated in the development of both coronary macrovascular and microvascular diseases (Belin de Chantemele & Stepp, 2012; Labazi & Trask, 2017; Pant et al., 2014; Pepine et al., 2015; Rocic, 2012). Therefore, we examined the effect of chloroquine on coronary endothelial function in control and diabetic mice. EDR, but not smooth muscle-dependent relaxation, was significantly attenuated in CAs of diabetic mice compared to CAs of control mice (Figure 3b,e). Interestingly, while chloroquine attenuated EDR in CAs from control mice (Figure 3c), it enhanced EDR in CAs isolated from diabetic mice (Figure 3d). The enhanced EDR in CAs from diabetic mice might be due to augmented EDH-dependent relaxation (Figure 3g).

EDR is usually caused by EDH and/or endothelium-dependent NO release. EDH-dependent relaxation is initiated by membrane hyperpolarization in ECs that can evoke SMC hyperpolarization by intercellular communication through gap junctions. EDH-dependent relaxation can also be induced by releasing EDHFs (e.g., EETs,  $H_2O_2$ , and anandamide). We and other investigators demonstrate that the activity of endothelial gap junction is attenuated in diabetes (Makino et al., 2008; Makino et al., 2015; Roy, Jiang, Li, & Kim, 2017). Figure 3k demonstrates that pretreatment of 18GA (a gap junction inhibitor) significantly inhibits chloroquine-induced augmentation of EDH-dependent vascular relaxation in diabetic mice. These data suggest that increased gap junction activity is involved in enhanced EDH-dependent relaxation by chloroquine in diabetes. Furthermore, we directly measured gap junction activity and found that chloroquine does increase gap junction activity in diabetic MCECs (Figure 4a,b). Gap junctions are cell membrane channels made of connexin (Cx) proteins. ECs predominantly express Cx40, Cx37, and Cx43 (along with Cx45 and Cx32 in some organs; Brisset, Isakson, & Kwak, 2009; Cai et al., 2001; Esseltine & Laird, 2016; Figueroa & Duling, 2009; Hill et al., 2002; Hong & Hill, 1998; Okamoto et al., 2009; Sohl & Willecke, 2004; Yeh, Dupont, Coppin, Rothery, & Severs, 1997). We have observed

that Cx40 is highly expressed in coronary ECs in control mice but significantly down-regulated in diabetic ECs and the down-regulation of Cx40 is implicated in endothelial dysfunction in type 1 diabetes (Makino et al., 2008).

The  $t_{1/2}$  of Cxs, which is much shorter (1–5 hr) than other plasma membrane proteins, can be shortened or delayed by chemical treatments (Falk, Kells, & Berthoud, 2014). The degradation process of Cxs involves in autophagosome, where chloroquine tends to accumulate and inhibits various enzyme activities (Mauthe et al., 2018). It is thus possible that chloroquine will change Cx levels in ECs by altering Cx degradation. Indeed, Chen, Guo, et al. (2017) demonstrate that chloroquine attenuates the degradation of Cx40 in rats with brain injury. In this study, we treated CAs and MCECs with chloroquine only for 30 min. The short-term treatment with chloroquine may not be sufficient to affect the total amount of Cx proteins but may be enough to maintain Cxs in the plasma membrane (by reducing degradation and/or increasing trafficking) to increase the activity of gap junction. Further studies are required to examine the effects of chloroquine on Cx trafficking and degradation.

EDH-dependent vascular relaxation can be enhanced if gap junction activity is augmented and/or if ECs are more hyperpolarized by increasing activity of  $SK_{Ca}$  and  $IK_{Ca}$  channels. In this study, we did not measure membrane potential and the activity of  $SK_{Ca}$  and  $IK_{Ca}$  channels in MCECs. CPA-induced  $[Ca^{2+}]_{cyto}$  increase was significantly decreased by chloroquine treatment in control mice; however, chloroquine did not affect the response to CPA in diabetic MCECs (Figure 4c,d). These data imply that the activities of  $SK_{Ca}$  and  $IK_{Ca}$  channels were not altered by chloroquine treatment in diabetic MCECs. Even if chloroquine increases  $SK_{Ca}$  and  $IK_{Ca}$  channel activity in diabetic MCECs, this beneficial effect of chloroquine might not be translated well into vascular relaxation without improving gap junction activity by chloroquine. In Figure 4a,b, the activity of gap junction was significantly attenuated in MCECs of diabetic mice and chloroquine treatment restored gap junction activity. Therefore, increased EDH-dependent vascular relaxation by chloroquine in diabetic mice is likely due to restored gap junction activity by chloroquine in diabetic MCECs. In type 1 diabetic mice, we also observed that gap junction activity was attenuated in MCECs and the recovery of gap junction activity restored attenuated vascular relaxation (Makino et al., 2015). Therefore, the increase in gap junction activity by chloroquine would be an efficient way to restore vascular relaxation in diabetic mice.

Chloroquine is also believed to stimulate bitter taste receptor (TAS2R) and leads to vascular relaxation (Chen, Ping, et al., 2017; Manson et al., 2014; Sai et al., 2014). Chloroquine is known as an agonist of TAS2R3, TAS2R10, and TAS2R39 (Upadhyaya et al., 2014); therefore, it is natural to think that chloroquine regulates vascular tone through the activation of TAS2Rs. However, there is no study investigating whether the deletion of TAS2R inhibits chloroquine-induced vascular response. In addition, chloroquine-induced vascular relaxation is observed only at a high concentration ( $>10^{-4}$  M). This concentration is higher than the physiological concentration, which we could detect in the body after chloroquine

treatment for malaria. Many chemicals could directly contract or relax vessels at the high concentration. Due to uncertain mechanisms of chloroquine-mediated vascular response, we did not examine the direct effect of chloroquine, through this receptor, on coronary arterial response in current study.

In this study, we demonstrate that chloroquine attenuates EDR in CAs isolated from control mice but chloroquine enhances EDR in CAs from diabetic mice. The different outcome might result from the altered endothelial function in diabetic mice. The chloroquine-mediated attenuation of EDR, which was observed in CAs from control mice, is due partly to a decrease in endothelial NO production. The chloroquine-mediated increase in EDR is mainly due to the enhancement of EDH-dependent relaxation in diabetic CAs as a result of chloroquine-increased gap junction activity. The observations from this study indicate that chloroquine should be used with caution in patients with non-diabetic cardiovascular disease due to an adverse effect of chloroquine on coronary vascular function.

## ACKNOWLEDGEMENT

This work was supported by a grant from the National Heart, Lung, and Blood Institute of the National Institutes of Health (HL142214 and HL146764 to A. Makino).

## AUTHOR CONTRIBUTIONS

Q.Z. conducted the experiments, analysed the data and drafted and reviewed the manuscript. A.T., C.W., M.W., R.S., N.L., and Z.W. conducted the experiments and reviewed the manuscript. J.Y. and J.W. reviewed and edited the manuscript. A.M. conceived the project, designed the experiments, analysed the data, and reviewed and edited the manuscript.

## CONFLICT OF INTEREST

The authors declare no conflicts of interest.

## DECLARATION OF TRANSPARENCY AND SCIENTIFIC RIGOUR

This Declaration acknowledges that this paper adheres to the principles for transparent reporting and scientific rigour of preclinical research as stated in the *BJP* guidelines for [Design & Analysis](#), [Immunoblotting and Immunocytochemistry](#), and [Animal Experimentation](#), and as recommended by funding agencies, publishers and other organisations engaged with supporting research.

## ORCID

Jian Wang  <https://orcid.org/0000-0001-9537-2891>

Ayako Makino  <https://orcid.org/0000-0003-1259-8604>

## REFERENCES

- Alexander, S. P. H., Fabbro, D., Kelly, E., Marrion, N. V., Peters, J. A., Faccenda, E., ... CGTP Collaborators (2017). The Concise Guide to PHARMACOLOGY 2017/18: Enzymes. *British Journal of Pharmacology*, 174, S272–S359. <https://doi.org/10.1111/bph.13877>

- Alexander, S. P. H., Christopoulos, A., Davenport, A. P., Kelly, E., Marrion, N. V., Peters, J. A., ... CGTP Collaborators (2017). The Concise Guide to PHARMACOLOGY 2017/18: G protein-coupled receptors. *British Journal of Pharmacology*, 174, S17–S129. <https://doi.org/10.1111/bph.13878>
- Belin de Chantemele, E. J., & Stepp, D. W. (2012). Influence of obesity and metabolic dysfunction on the endothelial control in the coronary circulation. *Journal of Molecular and Cellular Cardiology*, 52, 840–847. <https://doi.org/10.1016/j.yjmcc.2011.08.018>
- Blazar, B. R., Whitley, C. B., Kitabchi, A. E., Tsai, M. Y., Santiago, J., White, N., ... Brown, D. M. (1984). In vivo chloroquine-induced inhibition of insulin degradation in a diabetic patient with severe insulin resistance. *Diabetes*, 33, 1133–1137. <https://doi.org/10.2337/diab.33.12.1133>
- Brisset, A. C., Isakson, B. E., & Kwak, B. R. (2009). Connexins in vascular physiology and pathology. *Antioxidants & Redox Signaling*, 11, 267–282. <https://doi.org/10.1089/ars.2008.2115>
- Cai, W. J., Koltai, S., Kocsis, E., Scholz, D., Schaper, W., & Schaper, J. (2001). Connexin37, not Cx40 and Cx43, is induced in vascular smooth muscle cells during coronary arteriogenesis. *Journal of Molecular and Cellular Cardiology*, 33, 957–967. <https://doi.org/10.1006/jmcc.2001.1360>
- Campbell, W. B., & Fleming, I. (2010). Epoxyeicosatrienoic acids and endothelium-dependent responses. *Pflügers Archiv*, 459, 881–895. <https://doi.org/10.1007/s00424-010-0804-6>
- Chen, G. F., & Suzuki, H. (1990). Calcium dependency of the endothelium-dependent hyperpolarization in smooth muscle cells of the rabbit carotid artery. *The Journal of Physiology*, 421, 521–534. <https://doi.org/10.1113/jphysiol.1990.sp017959>
- Chen, J. G., Ping, N. N., Liang, D., Li, M. Y., Mi, Y. N., Li, S., ... Cao, Y. X. (2017). The expression of bitter taste receptors in mesenteric, cerebral and omental arteries. *Life Sciences*, 170, 16–24. <https://doi.org/10.1016/j.lfs.2016.11.010>
- Chen, W., Guo, Y., Yang, W., Zheng, P., Zeng, J., & Tong, W. (2017). Involvement of autophagy in connexin 40 reduction in the late phase of traumatic brain injury in rats. *Brain Research Bulletin*, 131, 100–106. <https://doi.org/10.1016/j.brainresbull.2017.03.014>
- Cho, Y. E., Basu, A., Dai, A., Heldak, M., & Makino, A. (2013). Coronary endothelial dysfunction and mitochondrial reactive oxygen species in type 2 diabetic mice. *American Journal of Physiology. Cell Physiology*, 305, C1033–C1040. <https://doi.org/10.1152/ajpcell.00234.2013>
- Danquah, I., Bedu-Addo, G., & Mockenhaupt, F. P. (2010). Type 2 diabetes mellitus and increased risk for malaria infection. *Emerging Infectious Diseases*, 16, 1601–1604. <https://doi.org/10.3201/eid1610.100399>
- Egan, T. J. (2001). Structure-function relationships in chloroquine and related 4-aminoquinoline antimalarials. *Mini Reviews in Medicinal Chemistry*, 1, 113–123. <https://doi.org/10.2174/1389557013407188>
- Esseltine, J. L., & Laird, D. W. (2016). Next-generation connexin and pannexin cell biology. *Trends in Cell Biology*, 26, 944–955. <https://doi.org/10.1016/j.tcb.2016.06.003>
- Estrada, I. A., Donthamsetty, R., Debski, P., Zhou, M. H., Zhang, S. L., Yuan, J. X., ... Makino, A. (2012). STIM1 restores coronary endothelial function in type 1 diabetic mice. *Circulation Research*, 111, 1166–1175. <https://doi.org/10.1161/CIRCRESAHA.112.275743>
- Falk, M. M., Kells, R. M., & Berthoud, V. M. (2014). Degradation of connexins and gap junctions. *FEBS Letters*, 588, 1221–1229. <https://doi.org/10.1016/j.febslet.2014.01.031>
- Figuroa, X. F., & Duling, B. R. (2009). Gap junctions in the control of vascular function. *Antioxidants & Redox Signaling*, 11, 251–266. <https://doi.org/10.1089/ars.2008.2117>
- Fong, K. Y., & Wright, D. W. (2013). Hemozoin and antimalarial drug discovery. *Future Medicinal Chemistry*, 5, 1437–1450. <https://doi.org/10.4155/fmc.13.113>
- Fukao, M., Hattori, Y., Kanno, M., Sakuma, I., & Kitabatake, A. (1997). Sources of Ca<sup>2+</sup> in relation to generation of acetylcholine-induced endothelium-dependent hyperpolarization in rat mesenteric artery. *British Journal of Pharmacology*, 120, 1328–1334. <https://doi.org/10.1038/sj.bjp.0701027>
- Garland, C. J., & Dora, K. A. (2017). EDH: Endothelium-dependent hyperpolarization and microvascular signalling. *Acta Physiologica (Oxford, England)*, 219, 152–161. <https://doi.org/10.1111/apha.12649>
- Godo, S., Sawada, A., Saito, H., Ikeda, S., Enkhjargal, B., Suzuki, K., ... Shimokawa, H. (2016). Disruption of physiological balance between nitric oxide and endothelium-dependent hyperpolarization impairs cardiovascular homeostasis in mice. *Arteriosclerosis, Thrombosis, and Vascular Biology*, 36, 97–107. <https://doi.org/10.1161/ATVBAHA.115.306499>
- Harding, S. D., Sharman, J. L., Faccenda, E., Southan, C., Pawson, A. J., Ireland, S., ... NC-IUPHAR (2018). The IUPHAR/BPS guide to pharmacology in 2018: Updates and expansion to encompass the new guide to immunopharmacology. *Nucleic Acids Research*, 46, D1091–D1106. <https://doi.org/10.1093/nar/gkx1121>
- Hill, C. E., Rummery, N., Hickey, H., & Sandow, S. L. (2002). Heterogeneity in the distribution of vascular gap junctions and connexins: Implications for function. *Clinical and Experimental Pharmacology & Physiology*, 29, 620–625. <https://doi.org/10.1046/j.1440-1681.2002.03699.x>
- Hong, T., & Hill, C. E. (1998). Restricted expression of the gap junctional protein connexin 43 in the arterial system of the rat. *Journal of Anatomy*, 192(Pt 4), 583–593. <https://doi.org/10.1046/j.1469-7580.1998.19240583.x>
- Jarzyna, R., Kiersztan, A., Lisowa, O., & Bryla, J. (2001). The inhibition of gluconeogenesis by chloroquine contributes to its hypoglycaemic action. *European Journal of Pharmacology*, 428, 381–388. [https://doi.org/10.1016/S0014-2999\(01\)01221-3](https://doi.org/10.1016/S0014-2999(01)01221-3)
- Jeong, H. Y., Kang, J. M., Jun, H. H., Kim, D. J., Park, S. H., Sung, M. J., ... Lee, S. Y. (2018). Chloroquine and amodiaquine enhance AMPK phosphorylation and improve mitochondrial fragmentation in diabetic tubulopathy. *Scientific Reports*, 8, 8774. <https://doi.org/10.1038/s41598-018-26858-8>
- Kalia, S., & Dutz, J. P. (2007). New concepts in antimalarial use and mode of action in dermatology. *Dermatologic Therapy*, 20, 160–174. <https://doi.org/10.1111/j.1529-8019.2007.00131.x>
- Kilkenny, C., Browne, W., Cuthill, I. C., Emerson, M., & Altman, D. G. (2010). Animal research: Reporting *in vivo* experiments: the ARRIVE guidelines. *British Journal of Pharmacology*, 160, 1577–1579.
- Kim, J. H., & Saxton, A. M. (2012). The TALLYHO mouse as a model of human type 2 diabetes. *Methods in Molecular Biology*, 933, 75–87. [https://doi.org/10.1007/978-1-62703-068-7\\_6](https://doi.org/10.1007/978-1-62703-068-7_6)
- Kutner, S., Breuer, W. V., Ginsburg, H., & Cabantchik, Z. I. (1987). On the mode of action of phlorizin as an antimalarial agent in *in vitro* cultures of *Plasmodium falciparum*. *Biochemical Pharmacology*, 36, 123–129. [https://doi.org/10.1016/0006-2952\(87\)90389-3](https://doi.org/10.1016/0006-2952(87)90389-3)
- Labazi, H., & Trask, A. J. (2017). Coronary microvascular disease as an early culprit in the pathophysiology of diabetes and metabolic syndrome. *Pharmacological Research*, 123, 114–121. <https://doi.org/10.1016/j.phrs.2017.07.004>
- Larsson, B., & Tjalve, H. (1979). Studies on the mechanism of drug-binding to melanin. *Biochemical Pharmacology*, 28, 1181–1187. [https://doi.org/10.1016/0006-2952\(79\)90326-5](https://doi.org/10.1016/0006-2952(79)90326-5)

- Luo, S., Truong, A. H., & Makino, A. (2016). Isolation of mouse coronary endothelial cells. *Journal of Visualized Experiments*, 113, e53985. <https://doi.org/10.3791/53985>
- Mackenzie, A. H. (1983). Dose refinements in long-term therapy of rheumatoid arthritis with antimalarials. *The American Journal of Medicine*, 75, 40–45. [https://doi.org/10.1016/0002-9343\(83\)91269-X](https://doi.org/10.1016/0002-9343(83)91269-X)
- Makino, A., Dai, A., Han, Y., Youssef, K. D., Wang, W., Donthamsetty, R., ... Dillmann, W. H. (2015). O-GlcNAcase overexpression reverses coronary endothelial cell dysfunction in type 1 diabetic mice. *American Journal of Physiology. Cell Physiology*, 309, C593–C599. <https://doi.org/10.1152/ajpcell.00069.2015>
- Makino, A., Platoshyn, O., Suarez, J., Yuan, J. X., & Dillmann, W. H. (2008). Downregulation of connexin40 is associated with coronary endothelial cell dysfunction in streptozotocin-induced diabetic mice. *American Journal of Physiology. Cell Physiology*, 295, C221–C230. <https://doi.org/10.1152/ajpcell.00433.2007>
- Makino, A., Scott, B. T., & Dillmann, W. H. (2010). Mitochondrial fragmentation and superoxide anion production in coronary endothelial cells from a mouse model of type 1 diabetes. *Diabetologia*, 53, 1783–1794. <https://doi.org/10.1007/s00125-010-1770-4>
- Manson, M. L., Saffholm, J., Al-Ameri, M., Bergman, P., Orre, A. C., Sward, K., ... Adner, M. (2014). Bitter taste receptor agonists mediate relaxation of human and rodent vascular smooth muscle. *European Journal of Pharmacology*, 740, 302–311. <https://doi.org/10.1016/j.ejphar.2014.07.005>
- Mauthe, M., Orhon, I., Rocchi, C., Zhou, X., Luhr, M., Hijlkema, K. J., ... Reggiori, F. (2018). Chloroquine inhibits autophagic flux by decreasing autophagosome-lysosome fusion. *Autophagy*, 14, 1435–1455. <https://doi.org/10.1080/15548627.2018.1474314>
- Okamoto, T., Akiyama, M., Takeda, M., Gabazza, E. C., Hayashi, T., & Suzuki, K. (2009). Connexin32 is expressed in vascular endothelial cells and participates in gap-junction intercellular communication. *Biochemical and Biophysical Research Communications*, 382, 264–268. <https://doi.org/10.1016/j.bbrc.2009.02.148>
- O'Sullivan, S. E., Kendall, D. A., & Randall, M. D. (2004). Heterogeneity in the mechanisms of vasorelaxation to anandamide in resistance and conduit rat mesenteric arteries. *British Journal of Pharmacology*, 142, 435–442. <https://doi.org/10.1038/sj.bjp.0705810>
- Pant, R., Marok, R., & Klein, L. W. (2014). Pathophysiology of coronary vascular remodeling: Relationship with traditional risk factors for coronary artery disease. *Cardiology in Review*, 22, 13–16. <https://doi.org/10.1097/CRD.0b013e31829dea90>
- Pepine, C. J., Ferdinand, K. C., Shaw, L. J., Light-McGroary, K. A., Shah, R. U., Gulati, M., ... ACC CVD in Women Committee (2015). Emergence of nonobstructive coronary artery disease: A woman's problem and need for change in definition on angiography. *Journal of the American College of Cardiology*, 66, 1918–1933. <https://doi.org/10.1016/j.jacc.2015.08.876>
- Pestana, C. R., Oishi, J. C., Salistre-Araujo, H. S., & Rodrigues, G. J. (2015). Inhibition of autophagy by chloroquine stimulates nitric oxide production and protects endothelial function during serum deprivation. *Cellular Physiology and Biochemistry*, 37, 1168–1177. <https://doi.org/10.1159/000430240>
- Powrie, J. K., Shojaee-Moradie, F., Watts, G. F., Smith, G. D., Sonksen, P. H., & Jones, R. H. (1993). Effects of chloroquine on the dyslipidemia of non-insulin-dependent diabetes mellitus. *Metabolism*, 42, 415–419. [https://doi.org/10.1016/0026-0495\(93\)90096-7](https://doi.org/10.1016/0026-0495(93)90096-7)
- Rafikov, R., Fonseca, F. V., Kumar, S., Pardo, D., Darragh, C., Elms, S., ... Black, S. M. (2011). eNOS activation and NO function: structural motifs responsible for the posttranslational control of endothelial nitric oxide synthase activity. *The Journal of Endocrinology*, 210, 271–284. <https://doi.org/10.1530/JOE-11-0083>
- Reed, H., & Campbell, A. A. (1962). Central scotomata following chloroquine therapy. *Canadian Medical Association Journal*, 86, 176–178.
- Rees, R. B., & Maibach, H. I. (1963). Chloroquine: A review of reactions and dermatologic indications. *Archives of Dermatology*, 88, 280–289. <https://doi.org/10.1001/archderm.1963.01590210038006>
- Rocic, P. (2012). Why is coronary collateral growth impaired in type II diabetes and the metabolic syndrome? *Vascular Pharmacology*, 57, 179–186. <https://doi.org/10.1016/j.vph.2012.02.001>
- Roy, S., Jiang, J. X., Li, A. F., & Kim, D. (2017). Connexin channel and its role in diabetic retinopathy. *Progress in Retinal and Eye Research*, 61, 35–59. <https://doi.org/10.1016/j.preteyeres.2017.06.001>
- Sai, W. B., Yu, M. F., Wei, M. Y., Lu, Z., Zheng, Y. M., Wang, Y. X., ... Liu, Q. H. (2014). Bitter tastants induce relaxation of rat thoracic aorta precontracted with high K<sup>+</sup>. *Clinical and Experimental Pharmacology & Physiology*, 41, 301–308. <https://doi.org/10.1111/1440-1681.12217>
- Sanchez-Chapula, J. A., Salinas-Stefanon, E., Torres-Jacome, J., Benavides-Haro, D. E., & Navarro-Polanco, R. A. (2001). Blockade of currents by the antimalarial drug chloroquine in feline ventricular myocytes. *The Journal of Pharmacology and Experimental Therapeutics*, 297, 437–445.
- Sandow, S. L., & Hill, C. E. (2000). Incidence of myoendothelial gap junctions in the proximal and distal mesenteric arteries of the rat is suggestive of a role in endothelium-derived hyperpolarizing factor-mediated responses. *Circulation Research*, 86, 341–346. <https://doi.org/10.1161/01.RES.86.3.341>
- Smith, G. D., Amos, T. A., Mahler, R., & Peters, T. J. (1987). Effect of chloroquine on insulin and glucose homeostasis in normal subjects and patients with non-insulin-dependent diabetes mellitus. *British Medical Journal (Clinical Research Ed.)*, 294, 465–467. <https://doi.org/10.1136/bmj.294.6570.465>
- Sohl, G., & Willecke, K. (2004). Gap junctions and the connexin protein family. *Cardiovascular Research*, 62, 228–232. <https://doi.org/10.1016/j.cardiores.2003.11.013>
- Straub, A. C., Zeigler, A. C., & Isakson, B. E. (2014). The myoendothelial junction: Connections that deliver the message. *Physiology (Bethesda)*, 29, 242–249.
- Tona, L., Ng, Y. C., Akera, T., & Brody, T. M. (1990). Depressant effects of chloroquine on the isolated guinea-pig heart. *European Journal of Pharmacology*, 178, 293–301. [https://doi.org/10.1016/0014-2999\(90\)90108-I](https://doi.org/10.1016/0014-2999(90)90108-I)
- Tracey, W. R., & Peach, M. J. (1992). Differential muscarinic receptor mRNA expression by freshly isolated and cultured bovine aortic endothelial cells. *Circulation Research*, 70, 234–240. <https://doi.org/10.1161/01.RES.70.2.234>
- Upadhyaya, J. D., Singh, N., Sikarwar, A. S., Chakraborty, R., Pydi, S. P., Bhullar, R. P., ... Chelikani, P. (2014). Dextromethorphan mediated bitter taste receptor activation in the pulmonary circuit causes vasoconstriction. *PLoS ONE*, 9, e110373. <https://doi.org/10.1371/journal.pone.0110373>
- Wu, K., Zhang, Q., Wu, X., Lu, W., Tang, H., Liang, Z., ... Wang, J. (2017). Chloroquine is a potent pulmonary vasodilator that attenuates hypoxia-induced pulmonary hypertension. *British Journal of Pharmacology*, 174, 4155–4172. <https://doi.org/10.1111/bph.13990>
- Yeh, H. I., Dupont, E., Coppen, S., Rothery, S., & Severs, N. J. (1997). Gap junction localization and connexin expression in cytochemically identified endothelial cells of arterial tissue. *The Journal of Histochemistry and Cytochemistry*, 45, 539–550. <https://doi.org/10.1177/002215549704500406>
- Yuan, X., Xiao, Y. C., Zhang, G. P., Hou, N., Wu, X. Q., Chen, W. L., ... Zhang, G. S. (2016). Chloroquine improves left ventricle diastolic function in

streptozotocin-induced diabetic mice. *Drug Design, Development and Therapy*, 10, 2729–2737.

Zhang, D. X., Borbouse, L., Gebremedhin, D., Mendoza, S. A., Zinkevich, N. S., Li, R., & Gutterman, D. D. (2012). H<sub>2</sub>O<sub>2</sub>-induced dilation in human coronary arterioles: Role of protein kinase G dimerization and large-conductance Ca<sup>2+</sup>-activated K<sup>+</sup> channel activation. *Circulation Research*, 110, 471–480. <https://doi.org/10.1161/CIRCRESAHA.111.258871>

**How to cite this article:** Zhang Q, Tsuji-Hosokawa A, Willson C, et al. Chloroquine differentially modulates coronary vasodilation in control and diabetic mice. *Br J Pharmacol*. 2020;177:314–327. <https://doi.org/10.1111/bph.14864>